Eur Radiol (2007) 17: 1746–1762
DOI 10.1007/s00330-006-0491-z

MUSCULOSKELETAL

Bernard Mengiardi
Christian W. A. Pfirrmann
Juerg Hodler

Hip pain in adults: MR imaging appearance of common causes

Received: 27 March 2006
Revised: 25 August 2006
Accepted: 29 September 2006
Published online: 18 November 2006

B. Mengiardi (✉) ·
C. W. A. Pfirrmann · J. Hodler
Department of Radiology,
Orthopedic University Hospital
Balgrist,
Forchstrasse 340,
8008 Zurich, Switzerland
e-mail: mengiardi@yahoo.de
Tel.: +41-44-3863313
Fax: +41-44-3863319

Abstract To determine the exact origin of hip pain can be challenging. Symptoms apparently originating from the hip may arise from the pelvis, the sacroiliac joint, the lumbar spine, periarticular structures such as muscles and bursae, or from unexpected sites such as the abdominal wall, the genitourinary tract, or the retroperitoneal space. This article reviews the differential diagnosis of hip pain arising from the hip and surrounding structures and the role of different imaging methods with emphasis on magnetic resonance imaging where most recent advances have occurred.

Keywords MR imaging · Hip · Adults

Introduction

Symptoms relating to hip abnormalities are common. Approximately 2.5% of all sports-related injuries relate to the hip [1]. Furthermore, in the USA 14.3% of the adults aged 60 years or older reported hip pain on most days of the previous 6 weeks [2]. Hip pain is not uniform. It may be located in the groin, over the major trochanter, in the proximal thigh, or the buttock. Due to the complex anatomy of the hip and pelvis locating the exact origin of pain may be difficult. The pain may arise from the hip joint proper, but also from the pelvis, the lumbar spine, the sacroiliac joint, muscles and bursae about the hip joint, and even the abdominal wall, the genitourinary tract, or the retroperitoneal space. Although a careful clinical evaluation can mostly suggest the origin of pain, in some cases this may be difficult. Once the pain has been attributed to the hip, a large number of differential diagnoses have to be considered which determine the most suitable imaging method. Table 1 presents possible sources of hip pain subdivided by three major etiologies (acute trauma, sports-related injuries, and others) and by anatomical considerations.

Imaging modalities

Standard radiographs

Standard radiographs remain the basis for the evaluation of the adult hip. The standard views include an anteroposterior view of the pelvis and commonly a cross-table view of the symptomatic hips. Cross-table lateral views better display the anterosuperior portion of the femoral neck than the frog-leg view. This is an important consideration regarding the diagnosis of femoroacetabular impingement. In addition, in cases of a suspected fracture the cross-table lateral view should be ordered instead of the frog-leg view. For the evaluation of a dysplastic hip or of the joint space in osteoarthritis the so-called faux profil projection may be used alternatively [3].

Sonography

Sonography is widely available, quickly performed, and has proven to be sensitive and cost effective in the early detection and grading of muscle and tendon injuries and

Table 1 Possible diagnosis of hip pain in adults presented by origin of pain and history. *PVNS* pigmented villonodular synovitis

	Trauma	Sport-related injuries	Other abnormalities
Hip joint	Fracture	Labral tears	Degeneration
	Hip dislocation	Early manifestation of femoroacetabular impingement (FAI)	Labral tears
	Labral tears	Osteoarthritis	Femoroacetabular impingement
			Osteoarthritis
			Inflammatory conditions
			Septic arthritis
			Rheumatoid arthritis
			Spondylarthropathies
			Deposition disease
			Amyloid arthropathy
			Synovial abnormalities
			PVNS, chondromatosis,
			Sarcoma
Bone	Fracture	Fatigue fracture, e.g.	Transient osteoporosis
		Femoral neck	Insufficiency fracture
		Pubic ramus	Avascular necrosis of femoral head
		Avulsion fracture (young adults)	Tumors
		Anterosuperior iliac spine	Metastasis
		Anteroinferior iliac spine	Myeloma/lymphoma
		Hamstring avulsion	Primary bone tumors
		Osteitis pubis	
Muscles/tendons/bursae	Soft tissue contusion	Muscle strains	Tendinopathy
	Myositis ossificans	Tendinopathy	Abductor tendinopathy
		Adduction dysfunction	Bursitis (trochanteric, iliopsoas)
		Hamstrings avulsion	
		Bursitis (trochanteric, iliopsoas)	
Others		Snapping hip syndrome	
		Iliotibial band syndrome	
		Labral tears, loose body	
		Nerve compression	
		Piriformis syndrome ilioinguinal/obturator/	
		Lateral fem. cutan. nerve	
		Lumbar disc herniation	
		Sportsman's hernia	Genitourinary abnormalities

the presence of a bursitis [4]. In addition, sonography allows dynamic evaluation which is useful in patients with a snapping hip syndrome [5, 6] or in the context of suspected sportsmen's hernia [4, 7]; both entities will be discussed later. Commonly, sonography is performed to detect hip joint effusion, a common but relatively nonspecific sign of hip joint abnormalities including osteoarthritis, inflammatory disease, and others: a distance between the inner margins of the capsule and the cortex of the head-neck junction of 7 mm or more or a difference between both hips of 1 mm or more have been considered to represent "effusion" in the hip joint [8]. Another published cutoff level is 9 mm or more for hip joint effusion or synovitis [9]. However, not only joint effusion but also hypoechoic synovial proliferation may distend the anterior hip joint recess [10]. In heavy patients, internal echoes in the synovial space may be difficult to identify, and synovial proliferation can be difficult to differentiate from fluid based on their echogenicity. The presence of hyperemia on color or power Doppler imaging assists in differentiating the synovial membrane from effusion, although synovitis does not always present with hyperemia [10].

Computed tomography (CT)

Trauma is the main indication for performing CT in patients with hip pain. In an emergency setting, CT demonstrates fractures of the femoral neck which have not been detected on standard radiographs and are important for grading and surgical planning of complex fractures of the pelvis and proximal femur. In addition, CT is useful as a secondary investigation to demonstrate bone changes (e.g., osteoid osteoma), calcifications (e.g., chondrosarcoma), and ossifications. Multidetector CT is desirable because it more easily allows high-quality multiplanar and volumetric reformations [11, 12].

Magnetic resonance imaging (MRI)

Depending on the suspected origin of pain different imaging protocols of the hip region are appropriate. A first decision to make is whether to image both hips simultaneously or only the affected side. Imaging of both hips may be appropriate in suspected osteonecrosis or search for metastasis. In most other situations, single hip imaging provides better spatial and contrast resolution, due to the small field of view and the use of a dedicated surface coil.

At our institution, three different protocols are employed for imaging of the hip (Table 2). As for most joint protocols, three imaging planes are employed, and different types of sequences should be included. An oblique axial plane along the axis of the femoral neck is used by many radiologists because such images demonstrate femoral neck offset and may better demonstrate the acetabular labrum and acetabular cartilage when compared to standard axial images. Radial images of the labrum and acetabulum may improve the diagnosis of labral tears and better demonstrate abnormal waist of the femoral neck offset [13–15]. Direct radial acquisition of spin echo and other sequences is possible, but planning and viewing may be tedious depending on the available software. Radial imaging may suffer from image blurring and other artifacts including a hypointense stripe in the center of the radial slices. Using a transverse oblique three-dimensional (3D) gradient echo sequence with reformation of radial images using the long axis of the femoral neck as rotation axis may also serve the purpose of improving diagnostic performance of MR imaging for labral

Table 2 Suggestion for three protocols for MRI of the hip. *TR* repetition time, *TE* echo time, *Sth* slice thickness, *FOV* field of view, *SE* spin echo sequence, *TSE* turbo or fast spin echo sequence, *FISP* fast imaging with steady-state precession, *PD* proton density, *DESS* double-echo steady-state sequence, *FAI* femoroacetabular impingement, *STIR* short τ inversion recovery

	Possible indications	Plane	Sequence	TR (ms)	TE (ms)	Sth (mm)	FOV (mm)	Matrix
MRI hip general	E.g., osteonecrosis of femoral head	Coronal	T1w SE	534	14	3	160	512
		Coronal	T2w TSE fat sat	2,500	42	3	160	512
		Sagittal	T1w SE	350	14	4	160	512
		Sagittal	Water excitation 3D DESS	24	6.6	1.7	150	256
		Transverse oblique	Water excitation 3D true FISP	8.95	3.25	1.25	170	384
		If osteonecrosis: coronal both hips	T1w SE	505	12	4	400	512
MR arthrography hip	Labral tears, FAI, chondral lesions	Coronal	T1w SE	534	14	3	160	512
		Coronal	T2w TSE fat sat	2,500	42	3	160	512
		Sagittal	T1w SE	350	14	4	160	512
		Sagittal	3D DESS water excitation	24	6.6	1.7	150	256
		Transverse oblique *along axis of femoral neck*	3D DESS water excitation	24	11.8	1.25	170	512
				→ Radial reformations using the long axis of the femoral neck as rotation axis				
MRI abductor tendon, greater trochanter	Tendinopathies of abductor tendons, bursitis	Coronal *incl. greater trochanter*	T2w TSE	3,500	75	4	220	512
		Transverse *broad from the iliac crest incl. the greater trochanter*	T1w SE	600	12	6	180	512
		Transverse *over the greater trochanter*	STIR	5,500	68	4	180	512
		Sagittal *over the greater trochanter, not the joint*	T1w SE	510	14	3	140	512

tears and a shallow femoral head neck junction in femoroacetabular impingement.

In cases of suspected intra-articular abnormalities such as labral tears (e.g., in femoroacetabular impingement) or chondral lesions, direct MR arthrography is the modality of choice [16, 17].

For direct MR arthrography diluted MR contrast agents are used similarly to other joints, with concentrations of 2–4 mmol/l. The hip joint is typically injected from anteriorly. Beside the well-known injection site at the inferior junction between the femoral head and neck other injection sites have been described. The superolateral femoral head may be targeted or the central portion of the femoral neck [18].

If clinical data about the possible origin of pain are equivocal, one may consider starting the examination with two coronal sequences of the entire pelvis [e.g., a spin echo (SE) T1-weighted and a fluid-sensitive sequence such as short τ inversion recovery (STIR)] and then add three sequences with a smaller field of view (FOV) depending on the findings detected on the initial images [19].

Another variant which is rarely used in our patient population is intravenous injection of gadolinium-containing contrast. Enhanced sequences with or without fat suppression may be useful in suspected septic or systemic inflammation as well as in suspected neoplasms. Because contrast material appears in synovial fluid in diagnostically relevant amounts, intravenous injection also results in an arthrographic effect (indirect MR arthrography) which is occasionally used instead of direct MR arthrography. The disadvantage of indirect MR arthrography includes a lack of joint distension [20]. In addition, vascularized structures such as the labral base enhance after contrast injection. Differentiation between such enhancement and joint fluid entering due to detachment may be difficult.

MR imaging findings of common causes of hip pain

Hip joint

Labral tears

Labral lesions are a common cause of hip pain. In about half of the patients acetabular and femoral osseous abnormalities are found on standard radiographs, including a decreased head-neck waist, an aspherical femoral head, hip dysplasia, retroverted acetabulum, or osteoarthritis [21]. Most labral abnormalities are thought to be part of a continuum of morphological changes associated with hip deformities, resulting in labral tears, delamination of the adjacent cartilage, and, finally, early osteoarthritis [22, 23]. The most relevant etiologies of such changes are developmental dysplasia and femoroacetabular impingement [24].

MR arthrography is the modality of choice to assess the acetabular labrum with a sensitivity and accuracy of about 90% [25, 26]. Knowledge of anatomical variants is important for the correct interpretation of MR arthrography. Labral tears and labral detachment are most commonly located in the anterosuperior aspect of the acetabulum [22, 25, 26] seen as a linear contrast-filled structure within the hypointense labrum (Figs. 1, 2). It is a subject of debate if a sublabral sulcus representing a normal variant exists anterosuperiorly [26–30]. Adjacent to a degenerated or torn labrum paralabral cysts may be found [31] (Fig. 2), most typically seen anterosuperiorly or, less frequently, posterosuperiorly. On MR images these paralabral cysts are often lobulated or septated. Their size ranges from a few millimeters to up to 3 cm.

Femoroacetabular impingement (FAI)

FAI is clinically characterized by a history of painful internal rotation and a positive impingement test. During this test groin pain is provoked by a combined maneuver of 90° flexion, adduction, and internal rotation of the hip. FAI refers to a conflict between the proximal femur and the acetabular rim [23] and is a reason for premature osteoarthritis of the hip [32]. Two different types of FAI, the "cam" and the "pincer" type have been described [23].

In cam FAI an aspherical shape of the femoral head and a reduced depth of the femoral waist ("offset") leads to an abutment of the femoral head-neck junction against the acetabular rim [5]. In pincer impingement acetabular overcoverage leads to a conflict between the acetabulum

Fig. 1 Labral tear/detachment. MR arthrography of a 13-year-old boy with right-sided groin pain. The coronal T1-weighted sequence of the right hip demonstrates superior labral detachment with contrast-filled gap at the base (*arrowheads*)

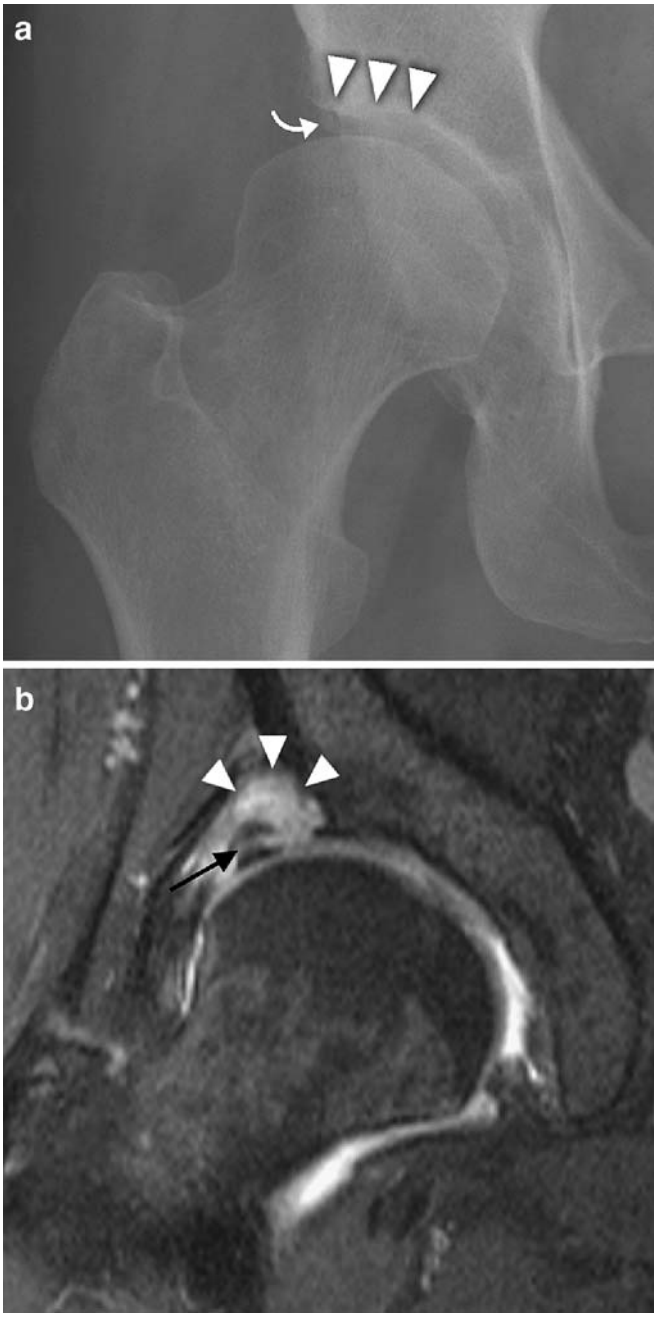

Fig. 2 Hip dysplasia with labral tear and paralabral ganglion. **a** Anteroposterior view of the right hip joint shows a mild dysplasia with insufficient acetabular coverage of the femoral head (*arrowheads*) and an os acetabuli (*curved arrow*). **b** On the coronal fat-suppressed T2-weighted images a large detached labrum with a horizontal tear (*black arrow*) and a paralabral ganglion cyst is visible (*arrowheads*)

and the femur. Labral tears and cartilage defects close to the abnormal labrum are commonly found in these joints [16, 23, 33]. In cam FAI the anteroposterior standard radiograph of the hip may demonstrate a so-called pistol-grip configuration with a flattened lateral femoral head-neck junction [34]. In addition, so-called synovial herniation, changes of the acetabulum, such as an os acetabuli [35], and ossification of the acetabular rim [36] may be seen. A reduced depth of waist of the head-neck junction anterosuperiorly is visible on cross-table lateral radiographs [37].

In pincer FAI the radiographs may demonstrate acetabular retroversion, coxa profunda, or acetabular protrusion resulting in an overcoverage of the femoral head [23, 38]. The crossover sign has been previously identified as a radiographic indicator of acetabular retroversion. It is considered to be present when the superior portion of the anterior acetabular rim is projected laterally relative to the posterior rim [39]. Projections of the acetabular fossa (in so-called coxa profunda) or the femoral head (in protrusio acetabuli) medial to the ilioischial line are radiographic indicators of increased acetabular socket depth.

MR arthrography is the modality of choice to quantify the reduced femoral waist [37] and at the same time to evaluate the labrum and cartilage. The extent of cartilage damage determines midterm outcome after surgical dislocation of the hip joint and surgical offset creation [40]. Typical MR findings in patients with cam FAI is a triad of reduced anterosuperior waist of the head-neck junction, anterosuperior labrum lesions, and adjacent cartilage damage [41] (Fig. 3). The reduced offset can be quantified by the so-called alpha angle which is determined on transverse images angled into the axis of the femoral neck. A cutoff angle of 55° has been found in a controlled study [37]. In the pincer type of FAI overcoverage of the femoral head may be diagnosed by measuring the acetabular depth which is larger than the head radius. There are labral lesions anterosuperiorly. The articular cartilage is damaged anterosuperiorly to posteroinferiorly (so-called contrecoup lesion) [41] (Fig. 4).

Osteoarthritis

Radiographically, joint space narrowing due to cartilage damage is seen, typically in the superior, load-bearing area. Less frequently, medial loss of joint space is seen, which may be associated with mild acetabular protrusion. Femoral and acetabular osteophytes, subchondral sclerosis, and subchondral cysts are typically present on standard radiographs. MR images also demonstrate labral degeneration, tears, and detachment as well as subchondral edema-like bone marrow changes. Thickening or buttressing of the medial femoral cortex may be apparent. In advanced osteoarthritis, standard radiographs are sufficient for the diagnosis and for surgical decision making. Additional imaging may be used in suspected early osteoarthritis with normal or nearly normal radiographs and for differential diagnostic purposes, for instance, for exclusion of avascular necrosis and radiographically occult stress fracture.

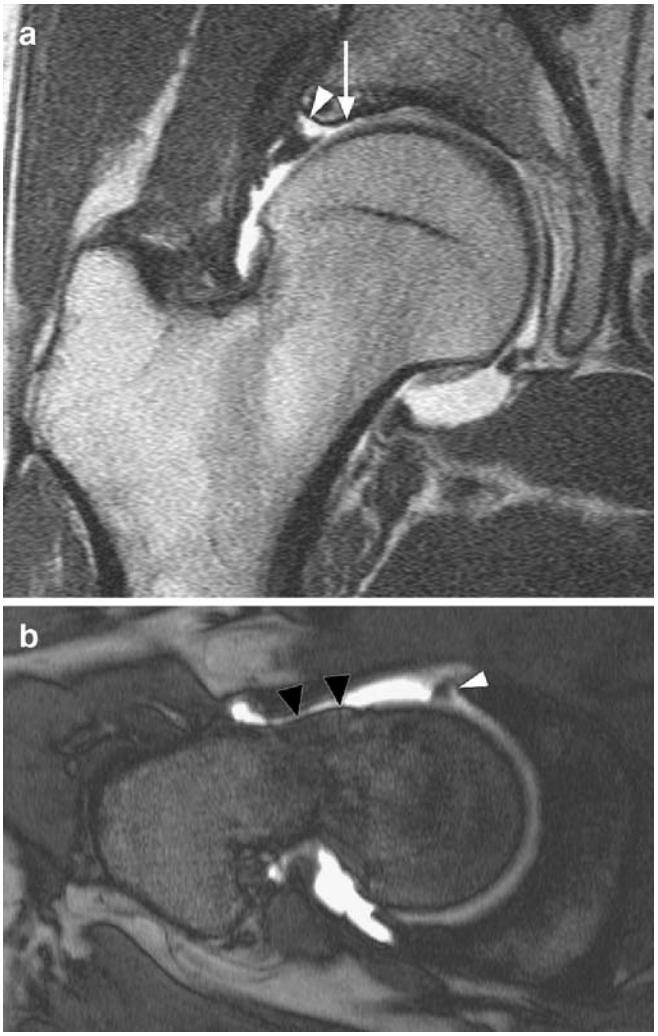

Fig. 3 Cam-type of femoroacetabular impingement (FAI). **a** On the coronal T1-weighted spin echo images (MR arthrogram obtained after injection of 10 ml of 2 mmol/l gadopentetate) superolateral labral detachment (*arrowhead*) and an adjacent cartilage defect at the acetabulum (*arrow*). **b** The angled axial gradient echo image reveals a reduced femoral waist ("offset") with a bony bump (*black arrowheads*)—a typical finding in cam-type FAI. In addition, a tear of the anterior labrum (*white arrowhead*) is visible

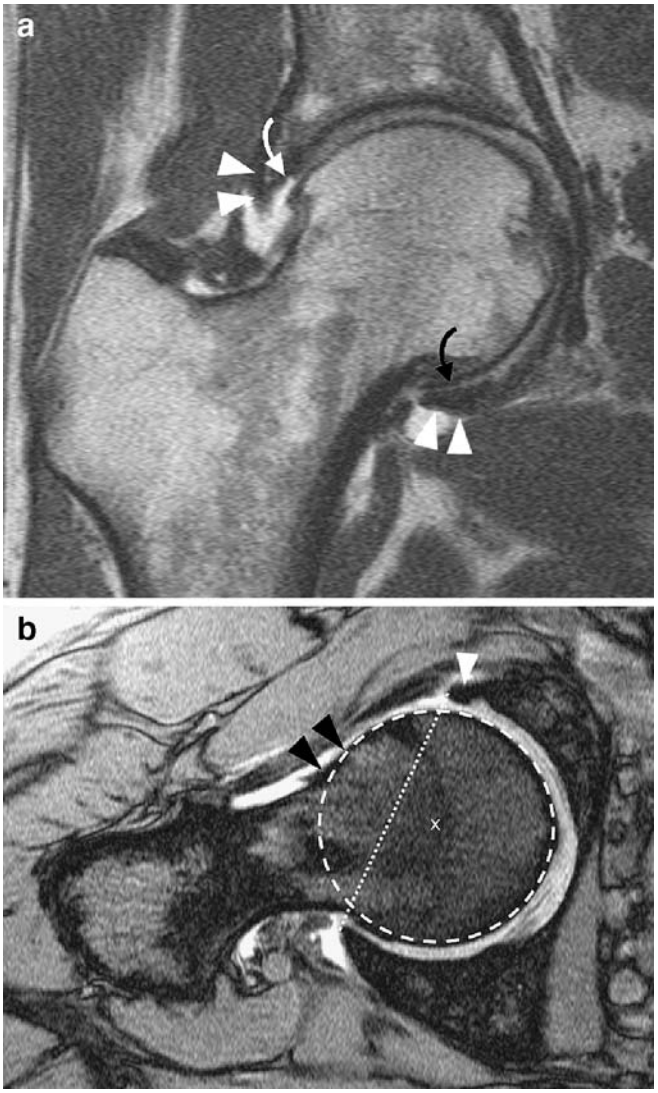

Fig. 4 Pincer-type of femoroacetabular impingement (FAI). **a** On the coronal T1-weighted spin echo image (MR arthrogram) protrusion of the femoral head is seen. The labrum is partially ossified at the base (*white arrows*) and cartilage defects are visible anterosuperiorly (*white curved arrow*) and posteroinferiorly (*black curved arrow*). **b** On the angled axial gradient echo sequences a normal offset of the head-neck junction (*black arrowheads*) is visible. Overcoverage of the femoral head is present when the center of the circumference of the head (*x*) is behind the line (*dotted line*) drawn from the anterior labrum (*white arrowhead*) to the posterior labrum

Rheumatoid arthritis (RA)

In RA inflammation and proliferation of the synovial membrane with or without bone erosion as well as intra-articular fluid collections are typically found. It affects all synovial structures, including tendon sheaths and bursae. Due to the commonly bilateral involvement of the hip joints in RA at least one fluid-sensitive sequence of the entire pelvis should be included in the MR imaging protocol.

On MR images, synovial thickening with low signal on T1-weighted images and high signal on T2-weighted or STIR sequences and effusion are typically found [42]. In active disease this pannus enhances strongly after intravenous injection of contrast. In chronic disease, pannus may become fibrotic. In addition, there may be deposits of hemosiderin, influencing MR signal characteristics (hypointense signal on all sequences). Detachment of fibrotic parts of the pannus from the synovial membrane leads to so-called rice bodies, which are demonstrated as hypointense filling defects within hyperintense joint fluid on T2-

weighted spin echo images. Their diameter is a few millimeters. Pannus may erode bone which most typically occurs at the central portion of the femoral head and acetabulum. Diffuse cartilage loss leads to superomedial migration of the femoral head, contrary to the typical superolateral migration found in cartilage damage associated with osteoarthritis. There may be a subchondral edema-like signal pattern. Subchondral cysts may be found [42].

Synovial chondromatosis

Synovial osteochondromatosis can be divided into a primary and secondary form. The primary synovial osteochondromatosis is an uncommon, benign disorder of unknown origin characterized by proliferation and metaplastic transformation of the synovial membrane, with formation of multiple cartilaginous or osteocartilaginous nodules within the joints, bursae, or tendon sheaths. The knee is the most commonly affected joint, followed by the elbow, hip, and shoulder [43]. This disease typically presents in the fourth or fifth decade.

Secondary osteochondromatosis occurs in association with trauma, osteoarthritis, osteonecrosis, and neuropathic arthropathy. In secondary osteochondromatosis, the intra-articular bodies tend to be larger, less numerous, and more varied in size than in the primary form. Secondary osteochondromatosis is typically associated with more pronounced degenerative disease of the joint [43].

On radiographs ossified or calcified juxta-articular bodies are present in about 80% of the involved joints. In half of the patients bone erosions and osteophytes are found, and in one-third of the patients joint space narrowing is present. MR imaging demonstrates synovial thickening (87%), bone erosions, and intra-articular bodies (73%) as well as synovial herniation (40%) [44]. Signal characteristics of unmineralized bodies are similar to hyaline cartilage. Ossified bodies may either be hypointense (in the presence of dense bone) or be hyperintense on T1-weighted images due to the presence of fatty bone marrow (Fig. 5).

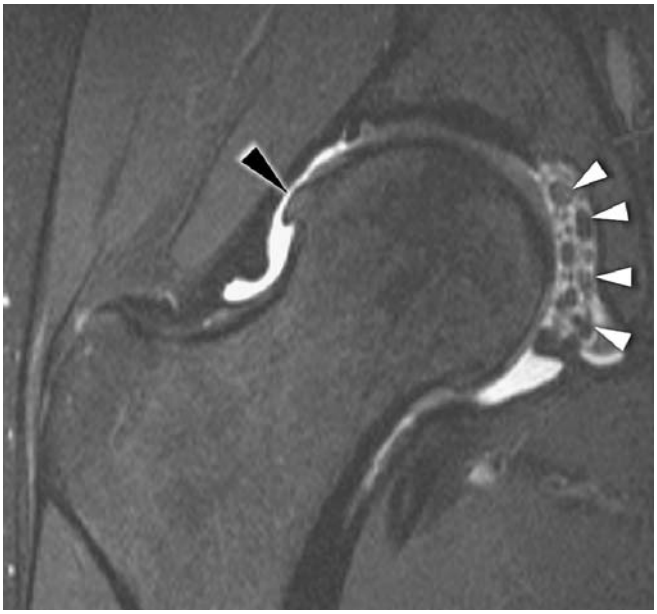

Fig. 5 Osteochondromatosis in osteoarthritis. On the fat-suppressed proton density-weighted image (MR arthrogram) multiple intra-articular mainly ossified bodies are visible in the acetabular notch (*white arrowheads*). *Black arrowhead*: femoral osteophyte in osteoarthritis

Pigmented villonodular synovitis (PVNS)

Pigmented villonodular synovitis is a benign proliferative disorder of the synovial membrane but tends to locally destruct the joint. Malignant transformation has been reported, although this is extremely rare and controversially discussed [45]. The hip joint is the second most commonly involved location after the knee (80% of cases) [43]. PVNS is usually seen in young adults, with a peak presentation in the third and fourth decades of life. Patients typically present with swelling, stiffness, and progressive pain in the involved joint. On standard radiographs advanced PVNS presents with multiple juxta-articular erosions, osteoarthritis, and arthritis-like changes [46]. MR imaging is the modality of choice for the assessment of PVNS. Typically, synovial-based nodules or masses with hypointense signal on both T1- and T2-weighted images are found. There may be a "blooming" artifact on gradient echo sequences due to the commonly present hemosiderin. There may be scattered areas of increased signal intensity seen on T1-weighted images which has been attributed to the presence of lipid-laden macrophages [47].

Bone abnormalities

Fractures

This review article does not discuss acute fractures of the pelvis and femoral head and neck which are usually diagnosed on radiographs or computed tomography. Occult fractures are well displayed by MR imaging. These fractures merit a review of their own due to the importance of the subject both in the orthopedic and radiological literature and because the use of imaging is quite different from the type of abnormalities discussed here. This article rather emphasizes radiographically occult and stress-related fractures.

Stress fractures can be divided into fatigue and insufficiency fractures. Fatigue fractures result from abnormal stress to normal bone and are common in athletes such as runners and jumpers [48]. In the pelvis and hip region, the

proximal femur is the most typical location, followed by the pubic rami [49]. Femoral fatigue fractures typically occur at the medial portion (compressive surface) of the femoral neck (Fig. 6), whereas insufficiency fractures often occur at the lateral portion of the femoral neck where tensile forces are most pronounced.

Insufficiency fractures result from normal stress to abnormal bone. They are most commonly seen in elderly women suffering from osteoporosis, but also in hyperparathyroidism, osteomalacia, osteogenesis imperfecta, and rickets as well as in individuals who have undergone pelvic irradiation. The most common locations are subcapital, femoral neck, intertrochanteric, sacral, supra-acetabular, pubic body, and pubic rami.

These fractures are commonly radiographically occult. MR imaging is a fast and cost-effective method in the diagnosis of such abnormalities, with an accuracy of 100% [50]. If occult fractures are expected, some authors have suggested using a limited low-cost study using only a T1-weighted sequence of the pelvis [51]. In accordance with others [52] we use an additional fluid-sensitive sequence in order to distinguish bone sclerosis from active bone remodeling.

In stress fractures MR imaging demonstrates edema-like abnormalities or a fracture line (hypointense on both T1-weighted and fluid-sensitive sequences) at the predilection sites (Fig. 6). Although fatigue fractures can occur in the sacrum [49], this is the classic location for insufficiency fractures. These fractures are usually oriented parallel to the sacroiliac joints with edema-like changes [53–55]. If no fracture line is evident bone marrow abnormalities may mimic other diseases, such as avascular necrosis or metastatic disease, depending on neighboring structures. Computed tomography may assist in differentiating remodeling from osteolysis with trabecular destruction caused by neoplastic disease. Supra-acetabular insufficiency fractures have been described [56]. They show a line parallel to the acetabular roof, accompanied by surrounding bone marrow edema-like changes.

Transient osteoporosis of the hip (TOH)

This entity is typically seen in overweight middle-aged men and in women during the third trimester of pregnancy. TOH may be part of a continuum of bone marrow abnormalities including stress-related edema-like changes, subchondral fractures, and osteonecrosis [57–59]. On MR images an extensive bone marrow edema-like signal can be seen in the femoral head and neck, possibly associated with joint effusion. Such abnormalities are best seen on fluid-sensitive sequences. The absence of additional, circumscribed subchondral changes on T2-weighted or contrast-enhanced T1-weighted images has a 100% positive predictive value for the transient nature of the abnormality [60]. If circumscribed subchondral areas of low signal intensity are present

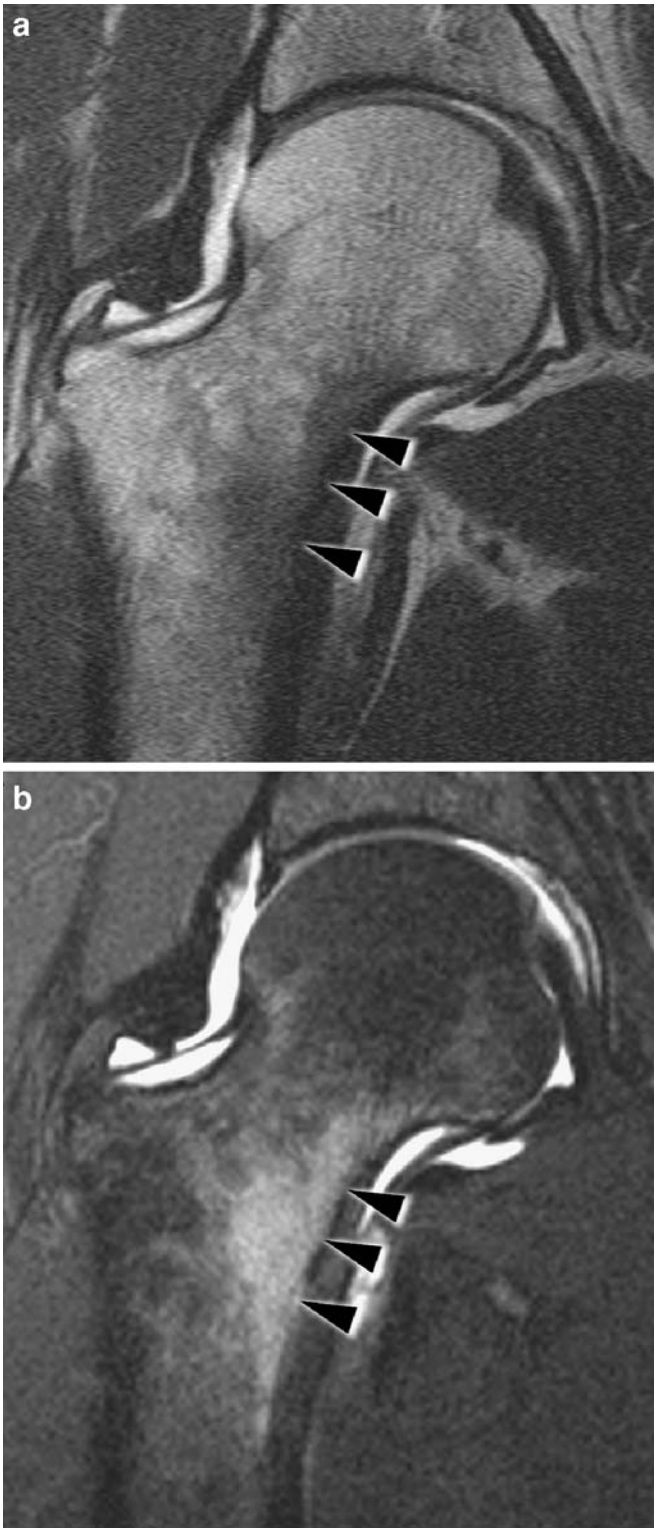

Fig. 6 Femoral neck stress reaction. MR arthrogram with **a** coronal T1-weighted spin echo image and **b** fat-suppressed T2-weighted turbo spin echo image. The medial femoral neck is the typical location for a stress reaction or fatigue fracture. In this case bone marrow edema-like abnormalities (*black arrowheads*) without a fracture line are visible

on both T1- and T2-weighted sequences the diagnosis of (irreversible) osteonecrosis is more probable. When the abnormality is 4 mm in thickness or more, there is a positive predictive value of 85% for irreversible diseases. When the abnormality is 12.5 mm or more in length, the positive predictive value is 73%. However, at follow-up, osteonecrosis was observed in only in 60% of such abnormalities [60].

Avascular necrosis (AVN) of the femoral head

MR imaging is the imaging modality of choice in suspected AVN of the femoral head [61, 62]. AVN occurs typically between the third and sixth decades of age and is more common in men than in women. Trauma with fracture of the femoral head or neck or hip dislocation are typical causes for AVN. Nontraumatic etiologies include corticosteroid use, alcohol abuse, sickle cell anemia, lupus erythematosus, coagulopathies, hyperlipidemia, and Gaucher's disease [63]. Commonly, no etiology can be determined. In contrast to standard radiography or CT, MR imaging is capable of detecting early stages of AVN with the possibility of early joint-sparing therapy such as core decompression. Typically, on T1-weighted images a serpiginous line of low signal surrounding an area of fatty marrow is seen in the anterosuperior femoral head (Fig. 7a). On T2-weighted images, a characteristic double line sign has been described [64]: parallel to the hypodense serpiginous line a hyperintense inner line is visible, representing granulation tissue at the interface of necrotic and viable bone (Fig. 7b). Due to the frequent bilateral occurrence of an AVN the contralateral hip must be evaluated. This may be done with an additional T1-weighted coronal sequence of both hips using the body coil. On standard radiographs, the existence of a crescent sign (subchondral fracture parallel to the articular surface) (Fig. 8) and collapse of the femoral head have been used as predictors for the outcome. With MR imaging, the assessment has become more precise. The extent measured in relation to the weight-bearing surface is relevant for the clinical outcome. The percentage of involved weight-bearing femoral area in relationship to the acetabular roof appears to be the most accurate parameter [65]. Clinical outcome is consistently poor for osteonecrosis involving more than 45% of the weight-bearing surface.

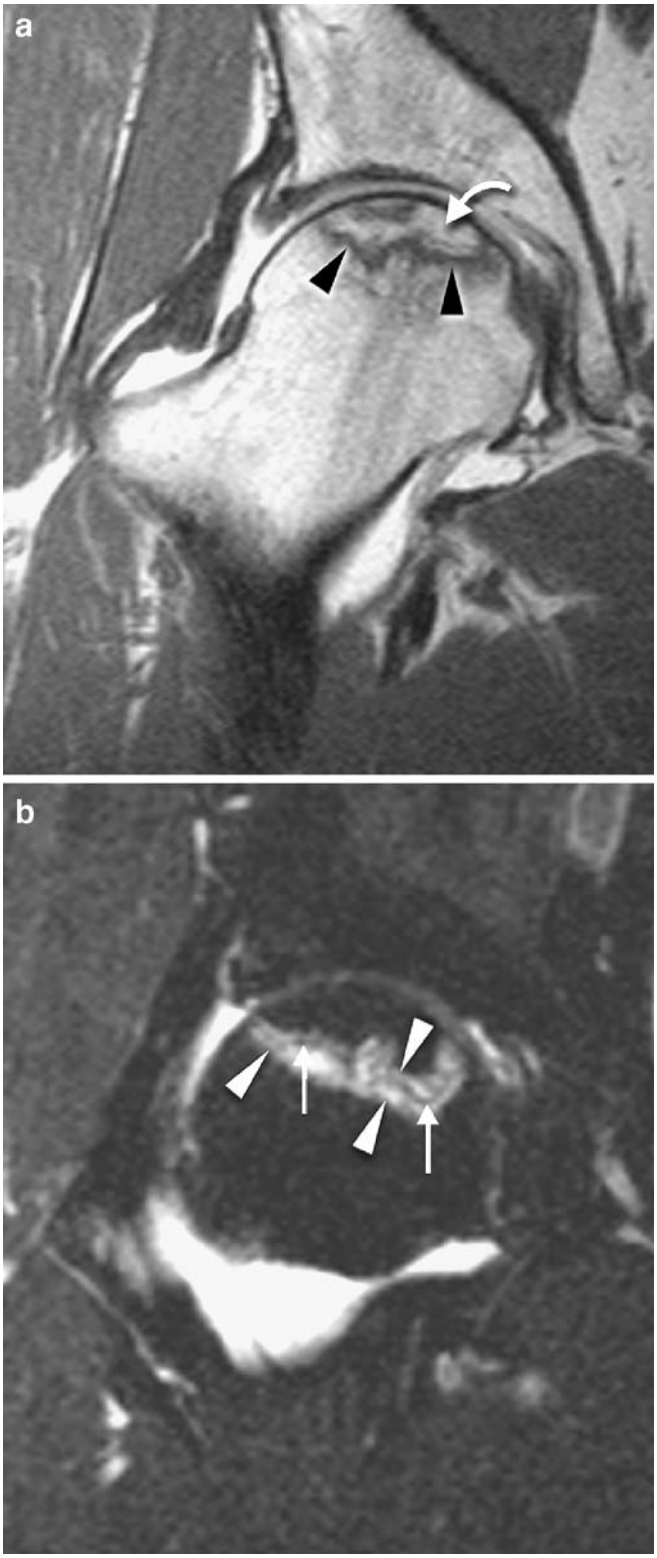

Fig. 7 MR arthrography findings in avascular necrosis of the femoral head. **a** On the T1-weighted spin echo image a serpiginous line of low signal (*arrowheads*) surrounding an area of fatty marrow (*curved arrow*) is seen anterosuperiorly. **b** On the fat-suppressed T2-weighted turbo spin echo image a hypodense serpiginous line (*arrows*) is paralleled by an inner and outer hyperintense line (*arrowheads*). These lines represent granulation tissue at the interface of necrotic and viable bone

Fig. 8 The crescent sign in an avascular necrosis of the femoral head. Radiographs reveal a subtle flattening of the superior portion of the femoral head with a subchondral fracture parallel to the articular surface (*solid arrows*). Note pistol grip configuration of the femoral head (*arrowheads*) which are related to a cam-type femoroacetabular impingement. *Open white arrow*: os acetabuli

Pubalgia—osteitis pubis

Within the fibrocartilaginous pubic symphysis a central cleft or cavity may be present. The importance of this cleft is not known [66]. The insertions of the adductor muscles and the gracilis muscle inferiorly as well as the conjoined tendon aponeurosis of the abdominal wall superiorly are close to the symphysis [66]. This anatomical complex is often responsible for groin pain in athletes. Potential diagnoses include osteitis pubis, adductor tendon or muscle overload, and posterior inguinal wall deficiency (sports hernia). So-called osteitis pubis is commonly encountered in fencers and runners as well as soccer and rugby players. Similar changes are seen with hormonally mediated ligamentous laxity in pregnant women [67]. Due to increased mechanical stress across the symphysis pubis, the ligamentous and capsular integrity of the joint is compromised and secondary degenerative changes with vertical instability may develop [68]. The altered biomechanics of the symphysis may lead to increased stress of the sacroiliac joint with associated degenerative changes or even sacral stress fractures [69]. The typical clinical history consists of unilateral pain located in the adductor region. Tenderness of the pubic symphysis (70%) and superior pubic ramus (40%) are the most consistent clinical signs [70]. In osteitis pubis standard radiographs demonstrate variable widening of the symphysis with cortical irregularities, erosions, sclerosis, and subchondral cysts [67]. Instability is suggested when widening is more than 7 mm or when the upper borders of the superior pubic rami have a vertical offset of more than 2 mm [71].

MR images demonstrate an irregular articular surface of the pubic bones, bone marrow signal abnormalities on each side of the symphysis, and subchondral cysts (Fig. 9). An osteophyte-like beak of the superior border of the pubic bone may be seen [72]. Increased signal on fluid-sensitive sequences is present within the symphysis and the adjacent soft tissue. A so-called secondary cleft has been described which is a linear structure contiguous with the primary (central) cleft of the symphysis [66]. This secondary cleft sign is best visualized on coronal STIR images and is observed at the inferior border of the symphysis and the pubic bone. The side of this secondary cleft corresponds to the side of the symptoms and may extend to the ipsilateral adductor and gracilis enthuses. So-called osteitis pubis and chronic adductor enthesopathy may be related [66].

An important differential diagnosis of osteitis pubis is *sportsman's hernia*. Alternatively, sports hernia, conjoined tendon tear, and Gilmore's hernia have been used for the same entity [68]. An imbalance of strong flexor and adductor muscles with weak abdominal muscles leading to laxity of the fascia transversalis, disruption of the conjoined tendon, and widening of the external inguinal ring may be the cause of sportsman's hernia. Pain is

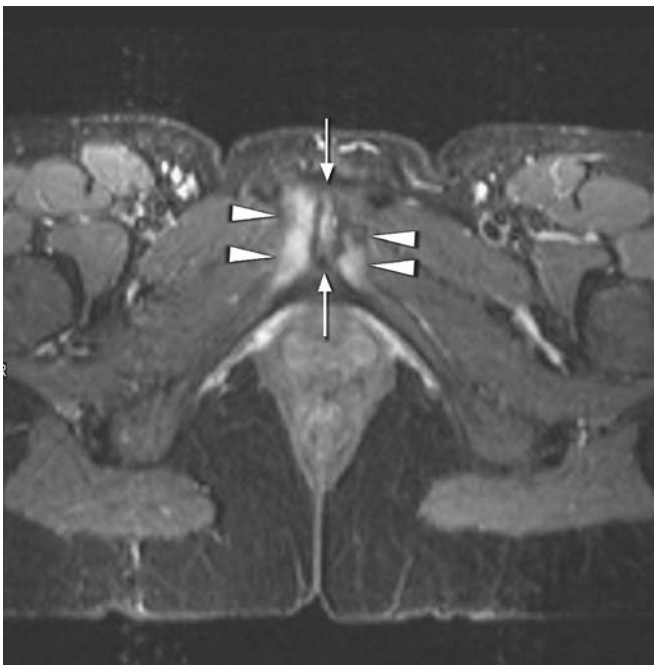

Fig. 9 MR imaging findings in osteitis pubis. On the axial STIR image of the pelvis the bone marrow signal abnormalities on each side of the symphysis (*arrowheads*) and increased signal within the symphysis (*arrows*) are present

typically absent at rest and provoked by activity such as sudden twisting movements. It may radiate into the thigh or testicles. A palpable bulge at this location may or may not be present. Unlike inguinal herniation there is no true herniation sac. Dynamic sonography of the inguinal ring appears to be the best imaging modality [4], demonstrating anterior bowing of the fascia transversalis and ballooning of the inguinal canal during the Valsalva maneuver [7]. MR imaging does not reliably demonstrate any abnormality in this diagnosis [68]. After surgical therapy resolution of symptoms has been reported in 87–97% [73, 74].

Bone tumors

Common tumors of the proximal femur are osteoid osteoma and osteoblastoma, chondroblastoma, chondrosarcoma, multiple myeloma, and metastasis [75]. In general, standard radiographs remain the most important image modality in the diagnosis of bone tumors and MR imaging is used to determine the extent of the tumor. CT is most useful in the assessment of bones in anatomically complex regions including the hip. CT may demonstrate cortical destruction and periosteal reaction. It may also demonstrate subtle matrix calcification not seen on standard radiographs, especially of the pelvis with its complex anatomy. The role of MR imaging is to evaluate the intramedullary and soft tissue extent of bone neoplasm, such as metastasis, myeloma, lymphoma, or giant cell tumor. In some types of tumors, characterization of the lesion is possible. In osteoid osteoma a small nidus surrounded by an edema-like signal is typically found and often CT is used to confirm the diagnosis. On MR imaging well-differentiated cartilaginous tumors may have a nodular appearance with high signal intensity on fluid-sensitive images and low signal foci representing calcification.

Muscles, tendons, and bursae

Muscle strain

Sonography has proved to be sensitive and cost effective in the early detection and grading of muscle injuries. However, MR imaging is often preferred to ultrasound because of the deep nature of the structures. Muscle strains typically involve the musculotendinous junction [76], occur during eccentric contraction, and are commonly seen in the rectus femoris muscle and in the hamstrings as well as the adductor longus and magnus muscles. Muscle injuries can be classified as follows on MR imaging [76, 77]. First-degree strains represent a minor degree of fiber disruption. Sonographically, a linear hypoechogenicity is seen within the muscle with loss of the normal pennated muscular architecture. On MR images interstitial edema with a feathery muscle pattern is visible (with or without hemorrhage, which may appear hypointense, depending on the stage of bleeding).

A second-degree strain corresponds to a partial tear without retraction. Part of the musculotendinous fibers is intact. On sonography, a hypoechogenic defect with disruption of the normal architecture is seen. Changes are more extensive than in first-degree strain and are often associated with hematoma with a heterogeneous echogenicity [4]. On MR images a hematoma with intra- and extramuscular fluid can be seen, typically at the musculotendinous junction.

A third-degree strain refers to a complete tear of the musculotendinous junctions with retraction. The retraction usually allows the diagnosis to be made clinically. MR imaging or sonography are useful to assess the extent of retraction.

Snapping hip syndrome

Snapping hip syndrome is a condition in which snapping or clicking sensations occur during movement of the hip, with or without associated pain. The causes of the snapping sensation can be intra- or extra-articular. The intra-articular form is most commonly caused by labral tears and less frequently by loose bodies within the hip joint [78].

The extra-articular causes have been divided into a lateral (or external) and a medial (or internal) type. The most common extra-articular causes are the iliotibial band or gluteus maximus snapping over the greater trochanter (lateral type) and the iliopsoas tendon snapping over the iliopectineal eminence of the pubic bone (medial type) [79]. Dynamic sonographic studies demonstrate the cause of extra-articular snapping hip in most patients [5, 6]. In a series of 54 patients with symptomatic internal snapping the diagnosis could be made using radiographs and sonography in 83% of the cases. The additional use of MR imaging allowed the correct diagnosis to be obtained in 100% of the cases. The authors concluded that radiographs and dynamic sonography should be used initially, reserving MR imaging for unresolved cases [6]. In our experience, although MR imaging lacks the dynamic capabilities of sonography, iliopsoas tendinosis or bursitis or a thickened iliotibial band may be visible as indirect signs of snapping hip. If an intra-articular snapping syndrome is expected, MR arthrography is our modality of choice.

Abnormalities of the abductors of the hip

Abductor abnormalities are a common cause of the so-called greater trochanter pain syndrome seen in middle-aged or elderly women [80]. Typically, the tendons of the gluteus medius and minimus are involved. The bony surface of the greater trochanter consists of four facets:

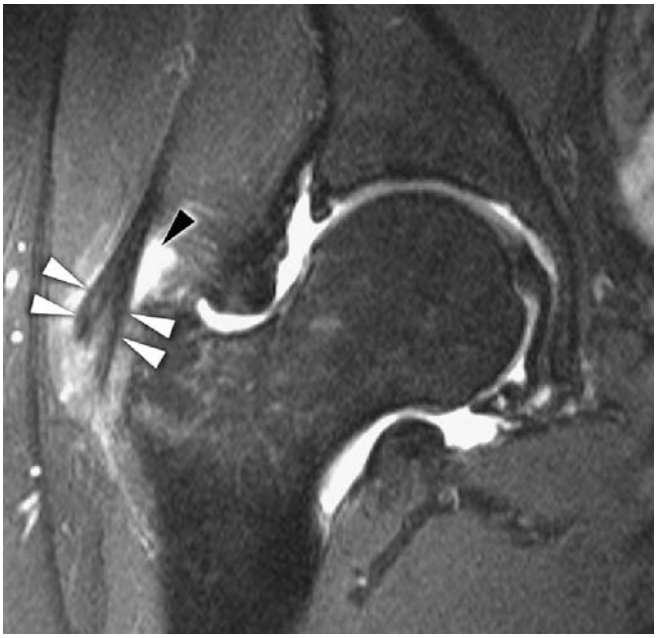

Fig. 10 Partial tear of the gluteus medius tendon. On the fat-suppressed T2-weighted turbo spin echo image the gluteus medius tendon demonstrates extensive thickening with increased signal (*white arrowheads*). In addition, bursitis of the medial subgluteal bursa is visible (*black arrowhead*)

anterior, lateral, posterior, and superoposterior [81]. The main tendon of the gluteus medius muscle attaches to the superoposterior facet, best seen on the sagittal and axial planes. The lateral portion of the gluteus medius tendon inserts on the lateral facet of the greater trochanter. The gluteus minimus muscle attaches to the anterior facet, best seen on axial and coronal images [81].

There may be tendinosis, partial and complete tears, and avulsion of the gluteus medius tendon from the trochanter [80, 82] (Figs. 10 and 11). Due to the superficial position of the tendons, sonography is useful in the diagnosis of abnormalities, with an 90% sensitivity and 95% specificity for the diagnosis of partial or complete tears of the gluteus medius and minimus tendons [83].

On MR images, partial tears are diagnosed by high signal intensity on fluid-sensitive sequences within the tendon that may have a normal diameter or may be thinned or thickened (Fig. 10). Bunker and co-workers [84] described the typical appearance of this tear as a circular or oval gluteus minimus tendon defect that extends

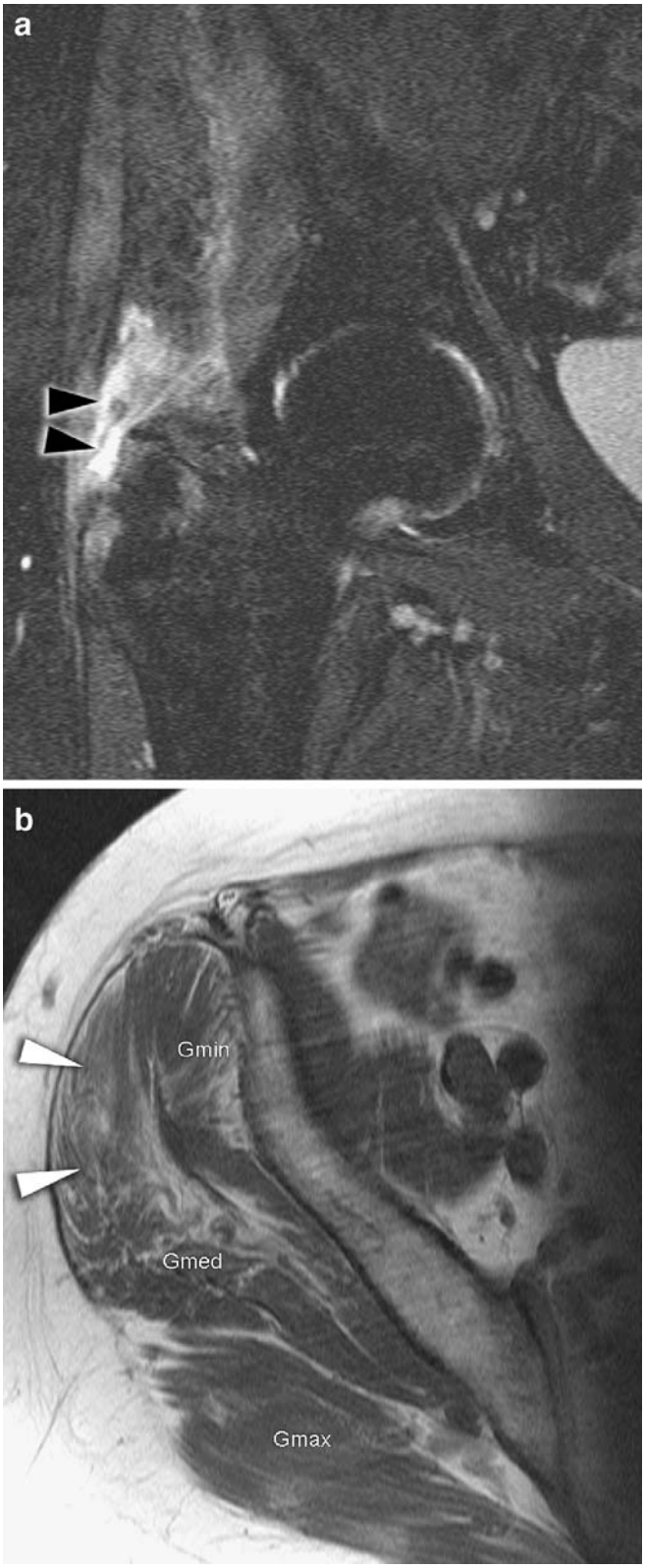

Fig. 11 MR imaging findings in a complete tear of the gluteus medius tendon. **a** The coronal fat-suppressed T2-weighted turbo spin echo image reveals a focal defect superior to the greater trochanter with fluid and edema (*arrowheads*), representing a complete tear of the gluteus medius tendon. **b** On the axial T1-weighted spin echo image of the pelvis, fatty degeneration of the anterior portion of the gluteus medius muscle is visible (*arrowheads*). *Gmin* gluteus minimus muscle, *Gmed* gluteus medius muscle, *Gmax* gluteus maximus muscle

posteriorly into the lateral part of the gluteus medius tendon. Focal areas of more than 1 cm in diameter superior to the greater trochanter are associated with tendon tears [85] (Fig. 11). Several studies have demonstrated that the pain associated with abductor tendon abnormalities responds poorly to conservative therapy, and surgical repair of tendon tears may lead to subsequent resolution of the symptoms [86].

Abnormalities of the abductor tendons and muscle are a common clinical problem after total hip arthroplasty (THA), especially if a transgluteal approach has been used. Although MR imaging played a minor role in the evaluation of symptomatic patients after THA, modifications of the sequences can reduce artifacts and optimize image quality. Spin echo sequences with high bandwidth, sequences with multiple refocusing pulses, and a frequency-encoding axis parallel to the long axis of the prosthesis are useful [87]. With such techniques, MR imaging is accurate in diagnosing abductor tendon abnormalities after THA [88, 89]. It is important to realize that many MR findings, such as altered signal and diameter of the tendons, bursal fluid collection, and fatty atrophy of the anterior two-thirds of the gluteus minimus muscle, are found in asymptomatic patients, although not as frequently as in symptomatic patients. However, defects of the abductor tendons and fatty atrophy of the gluteus medius muscle and the posterior part of the gluteus minimus muscle are uncommon in asymptomatic patients after THA and therefore appear to be clinically relevant [88].

Trochanteric bursitis

Trochanteric (subgluteus maximus, [81]) bursitis is another common cause of greater trochanteric pain and is difficult to distinguish from abductor tendon abnormalities clinically. Furthermore, bursitis has been reported in up to 40% of patients with lesions of the gluteus minimus and medius [87, 90]. Other less common causes of trochanteric bursitis include tuberculosis [91] and rheumatoid arthritis [92] as well as other systemic inflammatory diseases. On MR imaging, a fluid-filled bursa, possibly with septations and with enhancement of the wall after the intravenous administration of gadolinium, can be seen in trochanteric bursitis.

Fig. 12 MR imaging findings of hamstring avulsion injury with tendinosis of the semimembranous tendon. **a** Axial and **b** coronal fat-suppressed proton density-weighted turbo spin echo images. At the insertion of the semimembranous tendon anterolateral (*white arrowhead*) increased signal within the tendon, edema-like abnormalities of bone marrow (*open arrow*) and edema of the surrounding soft tissue (*curved arrow*) are visible. The conjoined tendon of the biceps femoris and the semitendinosus muscles (*black arrowhead*) is normal

Hamstring avulsion injuries and tendinopathy

Hamstring (biceps femoris, semitendinosus, and semimembranosus) avulsion injuries and tendinopathy may be seen in young athletes performing soccer, rowing, sprinting, and basketball. An avulsion injury may result from forceful eccentric muscle contraction or excessive passive lengthening [93]. However, it can also occur in gout, diabetes, hyperparathyroidism, and collagen vascular diseases [94]. Typically, the proximal conjoined tendons of the hamstring muscles at the posterolateral ischial tuberosity are involved. The semimembranous tendon originates anterolaterally of the conjoined tendon of the biceps femoris and the semitendinosus muscles. The spectrum of abnormalities includes tendinosis, partial and complete tear, and avulsion fractures [94, 95]. Avulsion fractures are quite rare and occur typically in adolescent athletes before closure of the tuberal apophysis. These

fractures are treated conservatively unless there is displacement of more than 2 cm [94]. In general, these avulsion fractures can be diagnosed on radiographs. If bone is intact, sonography or MR imaging may be used for the diagnosis. In acute hamstring injuries sonography only diagnosed 7 of 16 lesions correctly, whereas MR imaging correctly diagnosed all 16 avulsions [96]. The deep location of the ischial tuberosity, particularly in heavy patients, may render sonographic visualization difficult.

On MR images proximal hamstring tendinosis is seen as an increased intrasubstance signal, initially on T1-weighted images and later, in advanced tendinosis, on T2-weighted images (Fig. 12). Associated edema-like signal abnormalities may be present at the ischial tuberosity. More typically, the conjoined tendon of the semitendinosus and biceps femoris are affected [96]. In the case of a partial tear fluid-filled cleavage at the insertion is visible on fluid-sensitive sequences.

Conclusion

Hip pain in adults may have many different causes which may directly relate to the hip joint, to surrounding structures, or even to non-related structures such as the lumbar spine. Therefore, a clinical diagnosis should be made in order to perform appropriate imaging. Standard radiographs represent the basis for most hip-related diagnoses. The next step commonly consists of standard MR imaging or MR arthrography, although sonography may compete with MR imaging in many soft tissue-related abnormalities. A single MR imaging protocol is not sufficient for demonstration of all possible abnormalities of the hip. The early bilateral imaging protocols using the body or body array coils is no longer adequate considering the detailed analysis required by orthopedic surgeons. Although there remain some indications for bilateral examinations, most protocols should aim at optimal imaging of one hip, using dedicated coils and minimal field of view and slice thickness. Specialized imaging planes are useful. For evaluation of the labrum and articular cartilage direct arthrography is indicated. In the case of an inflammatory condition or a tumor, intravenous injection of gadolinium-containing contrast is indicated. Many other entities such as fractures, avascular osteonecrosis, transient osteoporosis, and osteitis pubis as well as muscle strains, tendinopathy, and bursitis can reliably be evaluated on unenhanced MR images using fluid-sensitive and T1-weighted sequences.

References

1. Anderson K, Strickland SM, Warren R (2001) Hip and groin injuries in athletes. Am J Sports Med 29(4): 521–533
2. Christmas C, Crespo CJ, Franckowiak SC, Bathon JM, Bartlett SJ, Andersen RE (2002) How common is hip pain among older adults? Results from the Third National Health and Nutrition Examination Survey. J Fam Pract 51(4):345–348
3. Lequesne MG, Laredo JD (1998) The faux profil (oblique view) of the hip in the standing position. Contribution to the evaluation of osteoarthritis of the adult hip. Ann Rheum Dis 57(11): 676–681
4. Miller TT (2005) Abnormalities in and around the hip: MR imaging versus sonography. Magn Reson Imaging Clin N Am 13(4):799–809
5. Pelsser V, Cardinal E, Hobden R, Aubin B, Lafortune M (2001) Extra-articular snapping hip: sonographic findings. AJR Am J Roentgenol 176(1):67–73
6. Wunderbaldinger P, Bremer C, Matuszewski L, Marten K, Turetschek K, Rand T (2001) Efficient radiological assessment of the internal snapping hip syndrome. Eur Radiol 11(9): 1743–1747
7. Orchard JW, Read JW, Neophyton J, Garlick D (1998) Groin pain associated with ultrasound finding of inguinal canal posterior wall deficiency in Australian Rules footballers. Br J Sports Med 32(2):134–139
8. Koski JM, Anttila PJ, Isomaki HA (1989) Ultrasonography of the adult hip joint. Scand J Rheumatol 18(2): 113–117
9. Sada PN, Rajan P, Jeyaseelan L, Washburn MC (1994) Standards for ultrasonographic measurements of the hip joint in Indian adults. Skeletal Radiol 23(2):111–112
10. Weybright PN, Jacobson JA, Murry KH, Lin J, Fessell DP, Jamadar DA et al (2003) Limited effectiveness of sonography in revealing hip joint effusion: preliminary results in 21 adult patients with native and postoperative hips. AJR Am J Roentgenol 181(1):215–218
11. Wedegartner U, Gatzka C, Rueger JM, Adam G (2003) Multislice CT (MSCT) in the detection and classification of pelvic and acetabular fractures (in German). Rofo 175(1):105–111
12. Harris JH Jr, Coupe KJ, Lee JS, Trotscher T (2004) Acetabular fractures revisited: part 2, a new CT-based classification. AJR Am J Roentgenol 182(6):1367–1375
13. Locher S, Werlen S, Leunig M, Ganz R (2002) MR-Arthrography with radial sequences for visualization of early hip pathology not visible on plain radiographs (in German). Z Orthop Ihre Grenzgeb 140(1):52–57
14. Kubo T, Horii M, Harada Y, Noguchi Y, Yutani Y, Ohashi H et al (1999) Radial-sequence magnetic resonance imaging in evaluation of acetabular labrum. J Orthop Sci 4(5):328–332

15. Plotz GM, Brossmann J, von Knoch M, Muhle C, Heller M, Hassenpflug J (2001) Magnetic resonance arthrography of the acetabular labrum: value of radial reconstructions. Arch Orthop Trauma Surg 121(8):450–457
16. Schmid MR, Notzli HP, Zanetti M, Wyss TF, Hodler J (2003) Cartilage lesions in the hip: diagnostic effectiveness of MR arthrography. Radiology 226(2):382–386
17. Toomayan GA, Holman WR, Major NM, Kozlowicz SM, Vail TP (2006) Sensitivity of MR arthrography in the evaluation of acetabular labral tears. AJR Am J Roentgenol 186(2):449–453
18. Duc SR, Hodler J, Schmid MR, Zanetti M, Mengiardi B, Dora C et al (2006) Prospective evaluation of two different injection techniques for MR arthrography of the hip. Eur Radiol 16(2):473–478
19. Zoga AC, Morrison WB (2005) Technical considerations in MR imaging of the hip. Magn Reson Imaging Clin N Am 13(4):617–634, v
20. Vahlensieck M, Peterfy CG, Wischer T, Sommer T, Lang P, Schlippert U et al (1996) Indirect MR arthrography: optimization and clinical applications. Radiology 200(1):249–254
21. Peelle MW, Della Rocca GJ, Maloney WJ, Curry MC, Clohisy JC (2005) Acetabular and femoral radiographic abnormalities associated with labral tears. Clin Orthop Relat Res 441: 327–333
22. McCarthy JC, Noble PC, Schuck MR, Wright J, Lee J (2001) The Otto E. Aufranc Award: the role of labral lesions to development of early degenerative hip disease. Clin Orthop Relat Res 393:25–37
23. Ganz R, Parvizi J, Beck M, Leunig M, Notzli H, Siebenrock KA (2003) Femoroacetabular impingement: a cause for osteoarthritis of the hip. Clin Orthop Relat Res 417:112–120
24. Leunig M, Podeszwa D, Beck M, Werlen S, Ganz R (2004) Magnetic resonance arthrography of labral disorders in hips with dysplasia and impingement. Clin Orthop Relat Res 418:74–80
25. Czerny C, Hofmann S, Neuhold A, Tschauner C, Engel A, Recht MP et al (1996) Lesions of the acetabular labrum: accuracy of MR imaging and MR arthrography in detection and staging. Radiology 200(1):225–230
26. Czerny C, Hofmann S, Urban M, Tschauner C, Neuhold A, Pretterklieber M et al (1999) MR arthrography of the adult acetabular capsular-labral complex: correlation with surgery and anatomy. AJR Am J Roentgenol 173(2):345–349
27. Walker JM (1981) Histological study of the fetal development of the human acetabulum and labrum: significance in congenital hip disease. Yale J Biol Med 54(4):255–263
28. Petersen W, Petersen F, Tillmann B (2003) Structure and vascularization of the acetabular labrum with regard to the pathogenesis and healing of labral lesions. Arch Orthop Trauma Surg 123(6):283–288
29. Hodler J, Yu JS, Goodwin D, Haghighi P, Trudell D, Resnick D (1995) MR arthrography of the hip: improved imaging of the acetabular labrum with histologic correlation in cadavers. AJR Am J Roentgenol 165(4):887–891
30. Petersilge C (2005) Imaging of the acetabular labrum. Magn Reson Imaging Clin N Am 13(4):641–652, vi
31. Magee T, Hinson G (2000) Association of paralabral cysts with acetabular disorders. AJR Am J Roentgenol 174(5):1381–1384
32. Wagner S, Hofstetter W, Chiquet M, Mainil-Varlet P, Stauffer E, Ganz R et al (2003) Early osteoarthritic changes of human femoral head cartilage subsequent to femoro-acetabular impingement. Osteoarthritis Cartilage 11(7):508–518
33. Ito K, Minka MA, 2nd, Leunig M, Werlen S, Ganz R (2001) Femoroacetabular impingement and the cam-effect. A MRI-based quantitative anatomical study of the femoral head-neck offset. J Bone Joint Surg Br 83(2):171–176
34. Stulberg SD, Cordell LD, Harris WH, Ramsey PL, MacEwen GD (1975) Unrecognized childhood hip disease: a major cause of idiopathic osteoarthritis of the hip. The Hip: Proceedings of the Third Open Scientific Meeting of the Hip Society 3. Mosby, St. Louis, pp 212–228
35. Kassarjian A, Yoon LS, Belzile E, Connolly SA, Millis MB, Palmer WE (2005) Triad of MR arthrographic findings in patients with cam-type femoroacetabular impingement. Radiology 236(2):588–592
36. Klaue K, Durnin CW, Ganz R (1991) The acetabular rim syndrome. A clinical presentation of dysplasia of the hip. J Bone Joint Surg Br 73(3):423–429
37. Notzli HP, Wyss TF, Stoecklin CH, Schmid MR, Treiber K, Hodler J (2002) The contour of the femoral head-neck junction as a predictor for the risk of anterior impingement. J Bone Joint Surg Br 84(4):556–560
38. Siebenrock KA, Schoeniger R, Ganz R (2003) Anterior femoro-acetabular impingement due to acetabular retroversion. Treatment with periacetabular osteotomy. J Bone Joint Surg Am 85(2):278–286
39. Reynolds D, Lucas J, Klaue K (1999) Retroversion of the acetabulum. A cause of hip pain. J Bone Joint Surg Br 81(2):281–288
40. Beck M, Leunig M, Parvizi J, Boutier V, Wyss D, Ganz R (2004) Anterior femoroacetabular impingement: part II. Midterm results of surgical treatment. Clin Orthop Relat Res 418:67–73
41. Pfirrmann CWA, Mengiardi B, Dora C, Kalberer F, Zanetti M, Hodler J (2006) MR arthrography in femoroacetabular impingement syndrome: characteristic findings in cam and pincer impingement in 50 patients. Radiology (in press)
42. Koulouris G, Morrison WB (2005) MR imaging of hip infection and inflammation. Magn Reson Imaging Clin N Am 13(4):743–755
43. Llauger J, Palmer J, Roson N, Bague S, Camins A, Cremades R (2000) Nonseptic monoarthritis: imaging features with clinical and histopathologic correlation. Radiographics 20 Spec No:S263–278
44. Kim SH, Hong SJ, Park JS, Cho JM, Kim EY, Ahn JM et al (2002) Idiopathic synovial osteochondromatosis of the hip: radiographic and MR appearances in 15 patients. Korean J Radiol 3(4):254–259
45. Kalil RK, Unni KK (1998) Malignancy in pigmented villonodular synovitis. Skeletal Radiol 27(7):392–395
46. Cotten A, Flipo RM, Chastanet P, Desvigne-Noulet MC, Duquesnoy B, Delcambre B (1995) Pigmented villonodular synovitis of the hip: review of radiographic features in 58 patients. Skeletal Radiol 24(1):1–6
47. Bancroft LW, Peterson JJ, Kransdorf MJ (2005) MR imaging of tumors and tumor-like lesions of the hip. Magn Reson Imaging Clin N Am 13(4): 757–774

48. Bencardino JT, Palmer WE (2002) Imaging of hip disorders in athletes. Radiol Clin North Am 40(2):267–287, vi–vii
49. Kiuru MJ, Pihlajamaki HK, Ahovuo JA (2003) Fatigue stress injuries of the pelvic bones and proximal femur: evaluation with MR imaging. Eur Radiol 13(3):605–611
50. Verbeeten KM, Hermann KL, Hasselqvist M, Lausten GS, Joergensen P, Jensen CM et al (2005) The advantages of MRI in the detection of occult hip fractures. Eur Radiol 15(1):165–169
51. Mlinek EJ, Clark KC, Walker CW (1998) Limited magnetic resonance imaging in the diagnosis of occult hip fractures. Am J Emerg Med 16(4): 390–392
52. Oka M, Monu JU (2004) Prevalence and patterns of occult hip fractures and mimics revealed by MRI. AJR Am J Roentgenol 182(2):283–288
53. Blomlie V, Lien HH, Iversen T, Winderen M, Tvera K (1993) Radiation-induced insufficiency fractures of the sacrum: evaluation with MR imaging. Radiology 188(1):241–244
54. Brahme SK, Cervilla V, Vint V, Cooper K, Kortman K, Resnick D (1990) Magnetic resonance appearance of sacral insufficiency fractures. Skeletal Radiol 19(7):489–493
55. Grangier C, Garcia J, Howarth NR, May M, Rossier P (1997) Role of MRI in the diagnosis of insufficiency fractures of the sacrum and acetabular roof. Skeletal Radiol 26(9):517–524
56. Otte MT, Helms CA, Fritz RC (1997) MR imaging of supra-acetabular insufficiency fractures. Skeletal Radiol 26(5):279–283
57. Turner DA, Templeton AC, Selzer PM, Rosenberg AG, Petasnick JP (1989) Femoral capital osteonecrosis: MR finding of diffuse marrow abnormalities without focal lesions. Radiology 171(1):135–140
58. Rafii M, Mitnick H, Klug J, Firooznia H (1997) Insufficiency fracture of the femoral head: MR imaging in three patients. AJR Am J Roentgenol 168(1):159–163
59. Guerra JJ, Steinberg ME (1995) Distinguishing transient osteoporosis from avascular necrosis of the hip. J Bone Joint Surg Am 77(4):616–624
60. Vande Berg BC, Malghem JJ, Lecouvet FE, Jamart J, Maldague BE (1999) Idiopathic bone marrow edema lesions of the femoral head: predictive value of MR imaging findings. Radiology 212(2):527–535
61. Coleman BG, Kressel HY, Dalinka MK, Scheibler ML, Burk DL, Cohen EK (1988) Radiographically negative avascular necrosis: detection with MR imaging. Radiology 168(2):525–528
62. Beltran J, Herman LJ, Burk JM, Zuelzer WA, Clark RN, Lucas JG et al (1988) Femoral head avascular necrosis: MR imaging with clinical-pathologic and radionuclide correlation. Radiology 166(1 Pt 1):215–220
63. Assouline-Dayan Y, Chang C, Greenspan A, Shoenfeld Y, Gershwin ME (2002) Pathogenesis and natural history of osteonecrosis. Semin Arthritis Rheum 32(2):94–124
64. Mitchell DG, Rao VM, Dalinka MK, Spritzer CE, Alavi A, Steinberg ME et al (1987) Femoral head avascular necrosis: correlation of MR imaging, radiographic staging, radionuclide imaging, and clinical findings. Radiology 162(3):709–715
65. Lafforgue P, Dahan E, Chagnaud C, Schiano A, Kasbarian M, Acquaviva PC (1993) Early-stage avascular necrosis of the femoral head: MR imaging for prognosis in 31 cases with at least 2 years of follow-up. Radiology 187(1):199–204
66. Brennan D, O'Connell MJ, Ryan M, Cunningham P, Taylor D, Cronin C et al (2005) Secondary cleft sign as a marker of injury in athletes with groin pain: MR image appearance and interpretation. Radiology 235(1):162–167
67. O'Connell MJ, Powell T, McCaffrey NM, O'Connell D, Eustace SJ (2002) Symphyseal cleft injection in the diagnosis and treatment of osteitis pubis in athletes. AJR Am J Roentgenol 179(4):955–959
68. Nelson EN, Kassarjian A, Palmer WE (2005) MR imaging of sports-related groin pain. Magn Reson Imaging Clin N Am 13(4):727–742
69. Major NM, Helms CA (1997) Pelvic stress injuries: the relationship between osteitis pubis (symphysis pubis stress injury) and sacroiliac abnormalities in athletes. Skeletal Radiol 26(12):711–717
70. Fricker PA, Taunton JE, Ammann W (1991) Osteitis pubis in athletes. Infection, inflammation or injury? Sports Med 12(4):266–279
71. Williams PR, Thomas DP, Downes EM (2000) Osteitis pubis and instability of the pubic symphysis. When nonoperative measures fail. Am J Sports Med 28(3):350–355
72. Gibbon WW, Hession PR (1997) Diseases of the pubis and pubic symphysis: MR imaging appearances. AJR Am J Roentgenol 169(3):849–853
73. Susmallian S, Ezri T, Elis M, Warters R, Charuzi I, Muggia-Sullam M (2004) Laparoscopic repair of "sportsman's hernia" in soccer players as treatment of chronic inguinal pain. Med Sci Monit 10(2):CR52–CR54
74. Hackney RG (1993) The sports hernia: a cause of chronic groin pain. Br J Sports Med 27(1):58–62
75. Beltran J, Opsha O (2005) MR imaging of the hip: osseous lesions. Magn Reson Imaging Clin N Am 13(4):665–676, vi
76. Steinbach LS, Fleckenstein JL, Mink JH (1994) Magnetic resonance imaging of muscle injuries. Orthopedics 17(11):991–999
77. Palmer WE, Kuong SJ, Elmadbouh HM (1999) MR imaging of myotendinous strain. AJR Am J Roentgenol 173(3):703–709
78. Yamamoto Y, Hamada Y, Ide T, Usui I (2005) Arthroscopic surgery to treat intra-articular type snapping hip. Arthroscopy 21(9):1120–1125
79. Shabshin N, Rosenberg ZS, Cavalcanti CF (2005) MR imaging of iliopsoas musculotendinous injuries. Magn Reson Imaging Clin N Am 13(4):705–716
80. Kingzett-Taylor A, Tirman PF, Feller J, McGann W, Prieto V, Wischer T et al (1999) Tendinosis and tears of gluteus medius and minimus muscles as a cause of hip pain: MR imaging findings. AJR Am J Roentgenol 173(4):1123–1126
81. Pfirrmann CW, Chung CB, Theumann NH, Trudell DJ, Resnick D (2001) Greater trochanter of the hip: attachment of the abductor mechanism and a complex of three bursae–MR imaging and MR bursography in cadavers and MR imaging in asymptomatic volunteers. Radiology 221(2):469–477

82. Chung CB, Robertson JE, Cho GJ, Vaughan LM, Copp SN, Resnick D (1999) Gluteus medius tendon tears and avulsive injuries in elderly women: imaging findings in six patients. AJR Am J Roentgenol 173(2):351–353
83. Connell DA, Bass C, Sykes CA, Young D, Edwards E (2003) Sonographic evaluation of gluteus medius and minimus tendinopathy. Eur Radiol 13(6):1339–1347
84. Bunker TD, Esler CN, Leach WJ (1997) Rotator-cuff tear of the hip. J Bone Joint Surg Br 79(4):618–620
85. Cvitanic O, Henzie G, Skezas N, Lyons J, Minter J (2004) MRI diagnosis of tears of the hip abductor tendons (gluteus medius and gluteus minimus). AJR Am J Roentgenol 182(1):137–143
86. Kagan A, 2nd (1998) Rotator-cuff tear of the hip. J Bone Joint Surg Br 80(1):182–183
87. Dwek J, Pfirrmann C, Stanley A, Pathria M, Chung CB (2005) MR imaging of the hip abductors: normal anatomy and commonly encountered pathology at the greater trochanter. Magn Reson Imaging Clin N Am 13(4):691–704, vii
88. Pfirrmann CW, Notzli HP, Dora C, Hodler J, Zanetti M (2005) Abductor tendons and muscles assessed at MR imaging after total hip arthroplasty in asymptomatic and symptomatic patients. Radiology 235(3):969–976
89. Twair A, Ryan M, O'Connell M, Powell T, O'Byrne J, Eustace S (2003) MRI of failed total hip replacement caused by abductor muscle avulsion. AJR Am J Roentgenol 181(6):1547–1550
90. Gordon EJ (1961) Trochanteric bursitis and tendinitis. Clin Orthop 20:193–202
91. Jaovisidha S, Chen C, Ryu KN, Siriwongpairat P, Pekanan P, Sartoris DJ et al (1996) Tuberculous tenosynovitis and bursitis: imaging findings in 21 cases. Radiology 201(2):507–513
92. Tanaka H, Kido K, Wakisaka A, Mine T, Kawai S (2002) Trochanteric bursitis in rheumatoid arthritis. J Rheumatol 29(6):1340–1341
93. Stevens MA, El-Khoury GY, Kathol MH, Brandser EA, Chow S (1999) Imaging features of avulsion injuries. Radiographics 19(3):655–672
94. Bencardino JT, Mellado JM (2005) Hamstring injuries of the hip. Magn Reson Imaging Clin N Am 13(4):677–690, vi
95. Koulouris G, Connell D (2005) Hamstring muscle complex: an imaging review. Radiographics 25(3):571–586
96. Koulouris G, Connell D (2003) Evaluation of the hamstring muscle complex following acute injury. Skeletal Radiol 32(10):582–589